Supporting information:

Visible-wavelength multiphoton activation confocal microscopy

Toshiki Kubo[1, 2], Kenta Temma[1, 2], Kazunori Sugiura[3], Hajime Shinoda[3], Kai Lu[3], Nicholas Isaac Smith[4], Tomoki Matsuda[3], Takeharu Nagai[3,5], and Katsumasa Fujita[1, 2, 5]*

[1]Department of Applied Physics, Osaka University, 2-1 Yamadaoka, Suita, Osaka 565-0871, Japan.

[2]Advanced Photonics and Biosensing Open Innovation Laboratory, AIST-Osaka University, Osaka University, 2-1 Yamadaoka, Suita, Osaka 565-0871, Japan

[3]The Institute of Scientific and Industrial Research (SANKEN), Osaka University, 8-1 Mihogaoka, Ibaraki, Osaka 567-0047, Japan

[4]Immunology Frontier Research Center, Osaka University, 3-1 Yamadaoka, Suita, Osaka 565-0871, Japan

[5]Transdimensional Life Imaging Division, Institute for Open and Transdisciplinary Research Initiatives, Osaka University, 2-1 Yamadaoka, Suita, Osaka 565-0871, Japan

* corresponding author: Katsumasa Fujita (fujita@ap.eng.osaka-u.ac.jp)

12 pages; 6 figures

Calculation of effective PSF of confocal microscopies

Equation S1 and S2 show the equations for the calculation of the effective PSFs of a confocal microscope with two-photon activation by either visible or NIR light (h_{MAC}) and a 1PE confocal microscope (h_{conf}), which are shown in Figure 1 in the main manuscript.

$$h_{MAC}(x,y,z) = h_{act}^2 \cdot h_{ex} \cdot (h_{det} \otimes \mathrm{D}) \quad \text{(S1)}$$

$$h_{conf}(x,y,z) = h_{ex} \cdot (h_{det} \otimes \mathrm{D}) \quad \text{(S2)}$$

Where h_{act} and h_{ex} are the activation and excitation PSF corresponding to the intensity distribution of the activation light at a wavelength of 560 nm or 800 nm and the excitation light at a wavelength of 488 nm, respectively. h_{det} shows the detection PSF of the system. In the calculation of PSFs, we used the vectorial diffraction theory[1] and assumed circular or random polarization. $\otimes$ represents 2D convolution in the detection (x', y') plane. D is the distribution of the sensitivity of the confocal detection as described in Equation S3. We assumed constant sensitivity inside of the radius of the pinhole r'_{d}.

$$\mathrm{D}(x',y') = \begin{cases} 1, & where\ x'^2 + y'^2 \le r_d'^2 \\ 0, & other\ wise \end{cases} \quad \text{(S3)}$$

In the case of the confocal with two-photon activation, the fluorescence emission is limited within the activated area. Therefore, the effective distribution of the fluorescence excitation, as shown in the middle column in Figure 1 in the main manuscript, is given by the product of the square of h_{act} and h_{ex}.

Estimation of switching efficiency

The investigation of switching efficiency was conducted by obtaining three confocal images under different activation and excitation conditions as shown in Figure S1. Then, the signal intensities in the obtained images were used to calculate the dependence of the switching efficiency on the intensities for two-photon activation by using the equation S4.

$$\frac{I_{\mathrm{sw}}(x,y)-I_{\mathrm{off}}(x,y)}{I_{\mathrm{on}}(x,y)-I_{\mathrm{off}}(x,y)} \propto \frac{\varepsilon_{\mathrm{on}}\, P_{488} C(x,y)\, A\big(P_{\mathrm{sw}}(y)\big) + \varepsilon_{\mathrm{off}}\, P_{488} C(x,y)\Big(1-A\big(P_{\mathrm{sw}}(y)\big)\Big) - \varepsilon_{\mathrm{off}}\, P_{488} C(x,y)}{\varepsilon_{\mathrm{on}}\, P_{488}\, C(x,y) - \varepsilon_{\mathrm{off}}\, P_{488}\, C(x,y)} = A\big(P_{\mathrm{sw}}(y)\big) \qquad \text{(S4)}$$

Where the density distribution of RSFPs is $C(x, y)$, the brightness of on-state and off-state RSFP under 488 nm excitation are $\varepsilon_{\mathrm{on}}$ and $\varepsilon_{\mathrm{off}}$, and the intensity of the pulsed laser and the 488 nm CW laser are P_{sw} and P_{488}, respectively. $I_{\mathrm{sw}}(x,y)$ is a signal intensity at each pixel of a confocal image obtained with spatially modulated activation intensities $P_{\mathrm{sw}}(y)$ as shown in Figure S1. Before the measurement of $I_{\mathrm{sw}}(x,y)$, the RSFPs were switched to the off state, and the confocal image obtained by 488 nm excitation after activation by the pulsed visible light presents the spatially modulated switching efficiency. However, since $I_{\mathrm{sw}}(x,y)$ also reflects the distribution of concentration of RSFP in the sample, it is necessary to normalize the signal $I_{\mathrm{sw}}(x,y)$ by the RSFPs distribution $I_{\mathrm{on}}(x,y)$. In addition, we need to consider the fluorescence signal from the RSFPs at the off-state and other background signals that cause an error in the estimation of the switching efficiency. Therefore, the distribution of the fluorescence from the off-state RSFPs $I_{\mathrm{off}}(x,y)$ was measured and subtracted from $I_{\mathrm{sw}}(x,y)$ and $I_{\mathrm{on}}(x,y)$ before calculating the switching efficiency as shown in Eq. S1

In our experiment, $I_{\mathrm{sw}}(x,y)$ was obtained with temporally-modulated activation and excitation lasers as shown in Figure S2. The fluorescence detection was temporally separated, and the

fluorescence signal under 488 nm excitation was considered as fluorescence the signal from RSFPs at on-state. However, as we discussed above, this procedure cannot remove the signal from the off-state RSFPs. As shown in Figure S3, the number of off-state RSFPs increases during the excitation of RSFPs by 488 nm laser, of which effect in the estimation of switching efficiency has to be considered. In our calculation, we subtracted $I_{sw}(x,y)$ *by* $I_{off}(x,y)$, and this calculation result corresponds to the fluorescence signal given in the area surrounded by the red line. This does not contain all the fluorescence signal from the on-state RSFPs. However, this does not affect the estimation of the switching efficiency since the ratio of extracted (red area) and missing (blue area) signal from on-sate RSFPs is the same in each pixel of the image. Therefore, we can estimate the dependence of the switching efficiency on the activation intensity by Eq. S1 without the effect of the fluorescence signal from off-state RSFPs.

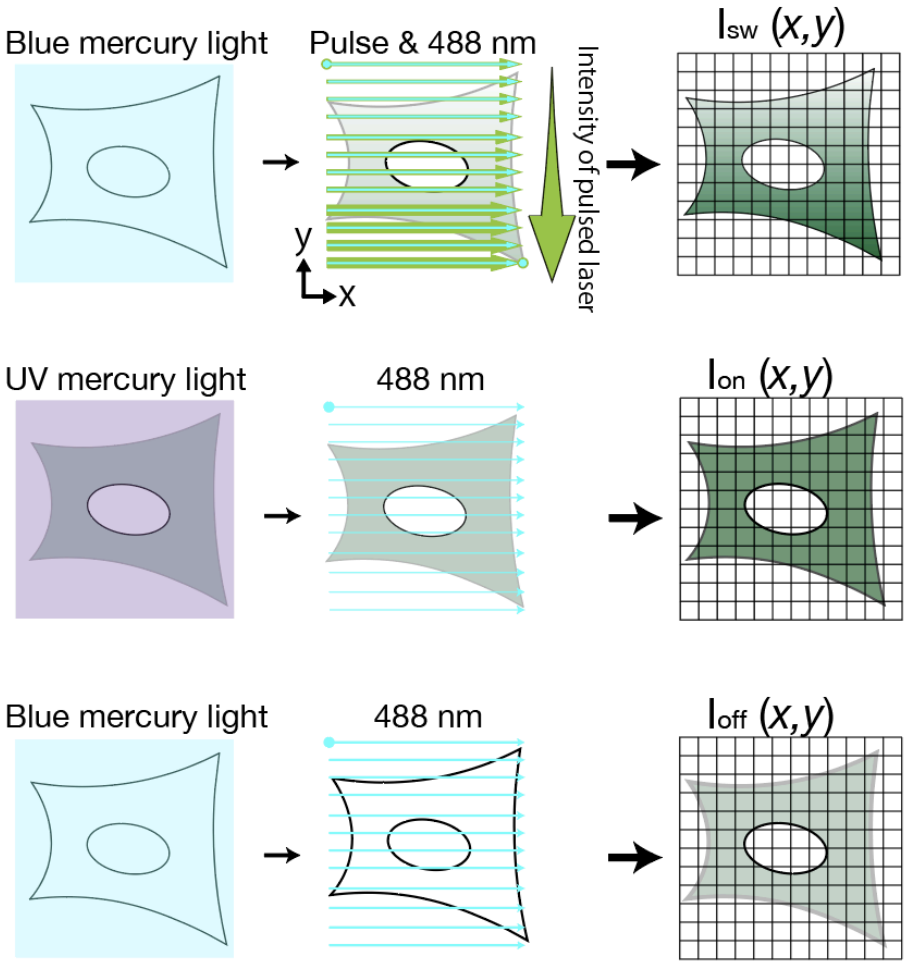

Figure S1. Schematic illustration of the irradiation process of the three confocal images obtained for the estimation of the switching efficiency response against the intensity of the pulsed laser.

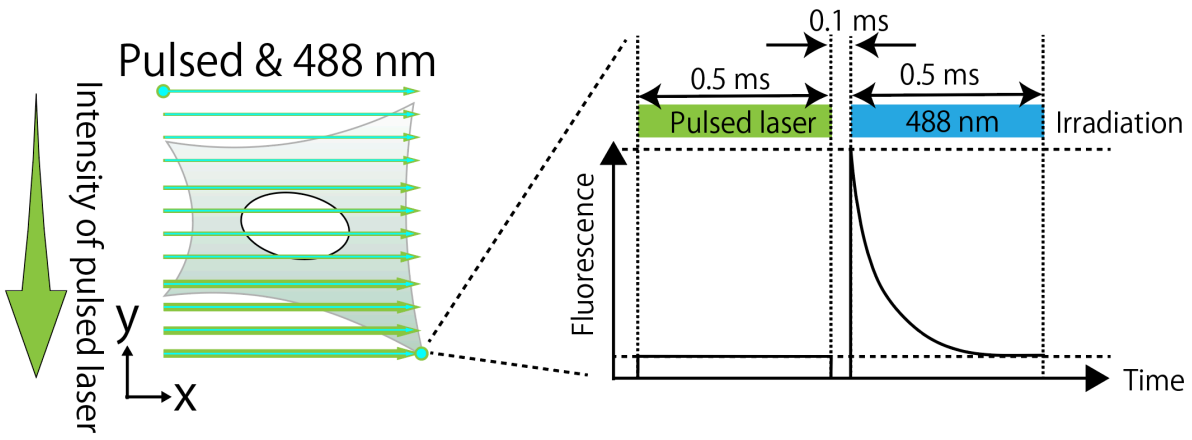

Figure S2. Schematic illustration of the modulation of the two lasers and an expected fluorescence signal in $I_{sw}(x,y)$.

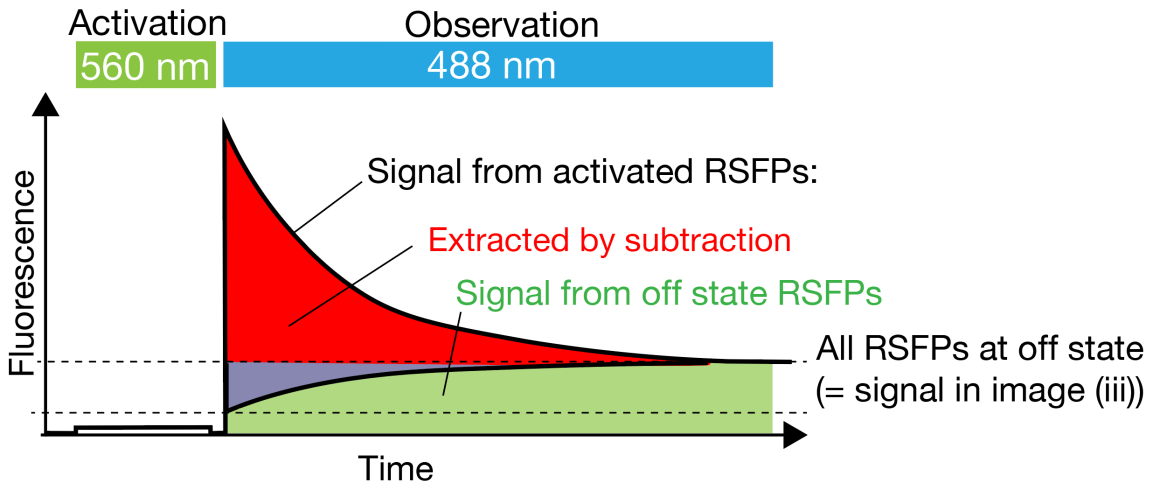

Figure S3. Fluorescence signal obtained at one pixel in $I_{sw}(x, y)$. A solid black line shows the expected fluorescence signal, which is composed of the fluorescence from either on- or off-state RSFPs, or both, as represented in the purple and green area, respectively. Since pulsed laser switches some RSFPs from off to on-state, the signal from the off-state RSFPs is the smallest at the beginning of the 488 nm irradiation. Since then 488 nm laser switches RSFPs from on- to off-state, the signal from off-state RSFPs gradually increases.

Procedure of the switching efficiency measurement

Here we show the procedure for estimating the switching efficiency in our experiment in Figure S4. To avoid light exposure at the same position of the samples during confocal imaging, the irradiation points are separated about 1 Airy Unit (AU), which was realized by setting the field of view to be 60 μm x 60 μm observed with the pixel number of 128 x 128.

(1) $I_{on}(x, y)$ was obtained. To switch all the RSFPs to on-state, widefield irradiation of UV light at 330 - 385 nm was applied to the sample and followed by confocal imaging with 488 nm excitation to obtain the distribution of RSFPs in the field of view. The pixel dwell time was set at 0.5 ms.

(2) $I_{off}(x, y)$ was obtained. Widefield irradiation of blue light with a wavelength range of 460-495 nm was applied to switch all the RSFPs to off-state, and confocal imaging with 488 nm excitation was performed to obtain the fluorescence intensity of fluorescent protein at off-state. The pixel dwell time was set at 0.5 ms.

(3) $I_{sw}(x, y)$ was obtained. We applied the widefield irradiation of blue light with a wavelength range of 460-495 nm again to switch all the RSFPs to off-state and obtained confocal fluorescence images with modulating the two lasers at each pixel as shown in Figure S2. At each pixel, initially, the pulsed laser was irradiated for 0.5 ms to activate RSFPs on samples. Just after the pulsed laser irradiation, an interval for 0.1 ms was set to avoid the overlap of the irradiation by the two lasers. After this, the 488 nm laser was irradiated 0.5 ms to excite RSFPs. The fluorescence signal was obtained only during the 488 nm irradiation. The activation of RSFPs by the pulsed laser was measured as the ratio of fluorescence signal from on- and off-state RSFPs. To know the relationship between the switching efficiency and the activation

intensity, the intensity of the pulsed light was increased every 4 lines in imaging to measure the switching efficiency at 32 different activation intensities.

Before the calculation using Eq. (S1), the obtained signal on each image was averaged at each area of 128 x 4 pixels, where the pulsed laser was irradiated with the same intensity. Then the switching efficiencies at each pulsed laser intensity are obtained by Eq. (S1) by using the averaged values. The averaged values have the information of switching efficiencies at each pulsed laser intensity. We plotted the averaged values against pulsed laser intensity in log-log scale (Figure S4).

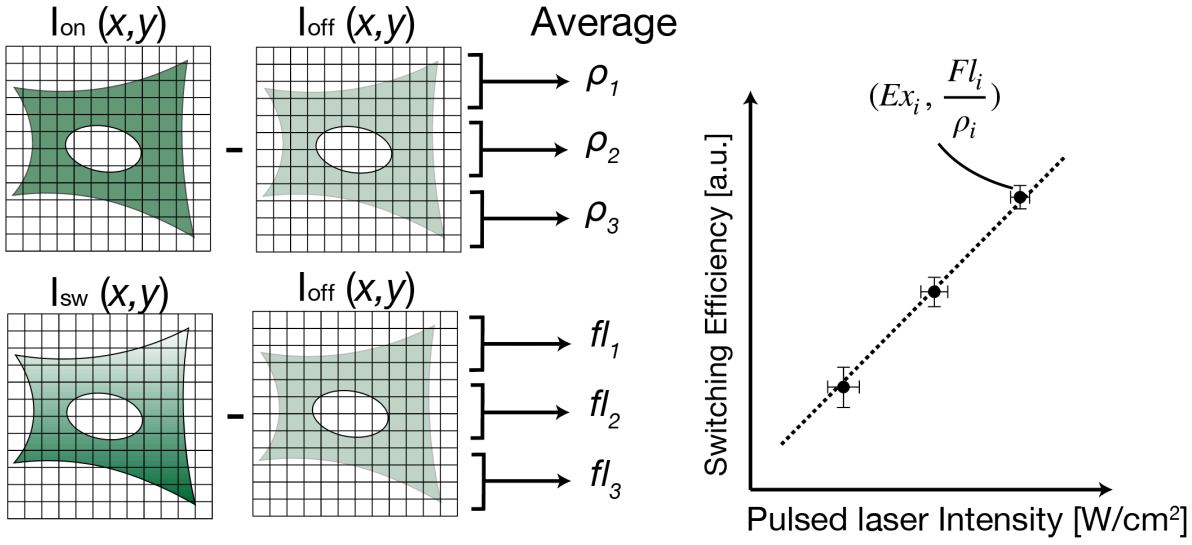

Figure S4. The analysis process of switching efficiency from obtained images. For simplification, we illustrated as if only 3 level intensities of pulsed laser were used, but in actual measurements, we used 32 levels of intensities. Ex_i represents the i-th level (i = 1, 2, …, 32) of the intensity of the pulsed laser. ρ_i and fl_i represent the average values of the fluorescence signal obtained in the area where the pulsed laser irradiated at an intensity of Ex_i in "$I_{on}(x,y) - I_{off}(x,y)$" and "$I_{sw}(x,y) - I_{off}(x,y)$", respectively.

Simulation of images of actin filament

To compare the theoretical and the experimental resolutions in Figure 5, we simulated effective PSFs and an image of an actin filament in vMAC and 1PE confocal microscopy as shown in Figure S5. The simulated images were calculated by convolution of the effective PSFs and an actin filament. We assumed an actin filament as a cylinder parallel to the y direction with a diameter of 8 nm, which is a typical diameter of actin filaments[2], and a length of 2 μm. In the x-direction, the filament is sufficiently small that the FWHM of the x-direction cross-section of the image is almost identical to the effective PSF of vMAC and 1PE. On the other hand, in the z-direction, the image obtained by 1PE is slightly blurred due to the actin structure elongated in the y-direction, whereas the image obtained by vMAC is unaffected due to signal localization caused by the nonlinear imaging property.

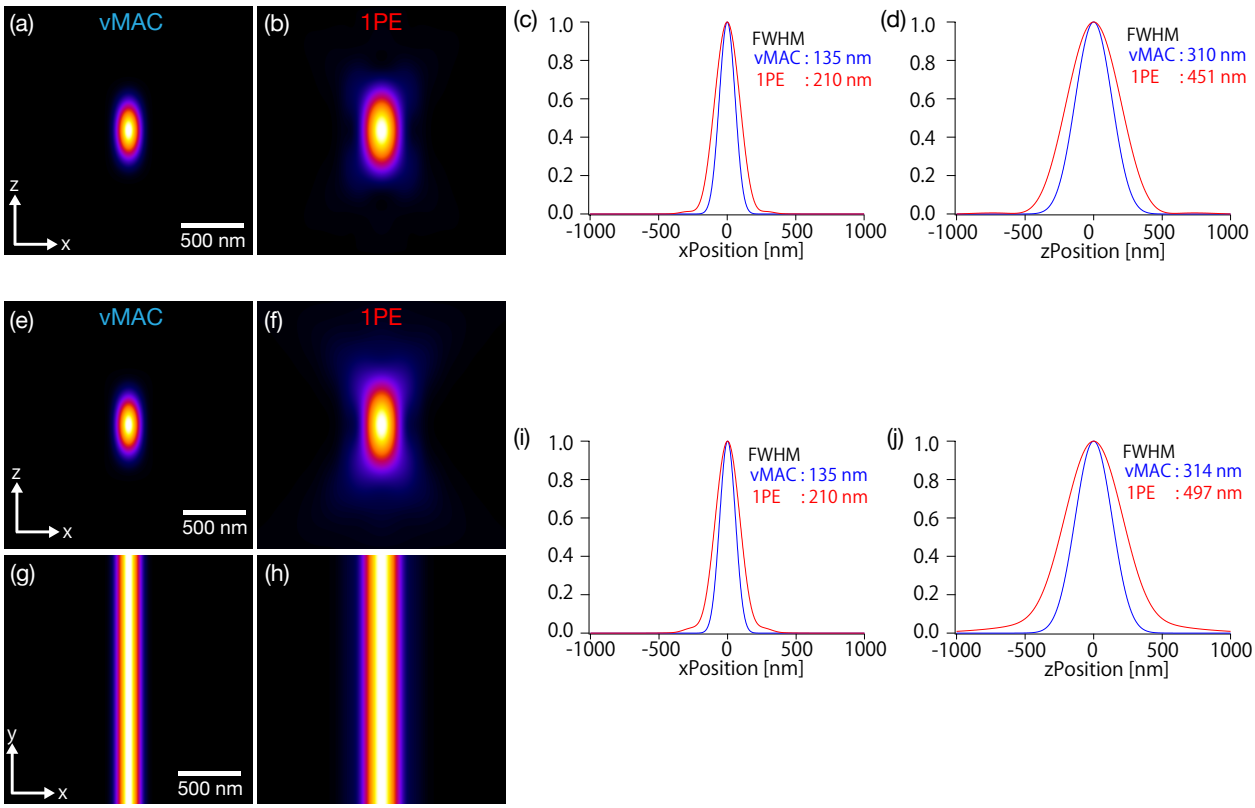

Figure S5. Calculation results of the effective PSFs (a)-(d) and images of an actin filament (e)-(j) in vMAC and 1PE confocal microscopy. The cross-sections of the effective PSFs in the x-z plane are shown for each in (a) and (b). The cross-sections of the simulated images in the x-z plane are shown for each in (e) and (f), and those in the x-y plane are shown in (g) and (h). The line profiles in the x and z direction are shown in (c) and (i), and (d) and (j), respectively.

Absorption spectra of RSFPs in off-state

Figure S6 shows the absorption spectra of the four species of RSFPs used in our experiment. The absorption peak wavelengths vary in order of shorter to longer as: rsEGFP2, Skylan-NS, Dronpa, and rsGamillus-S.

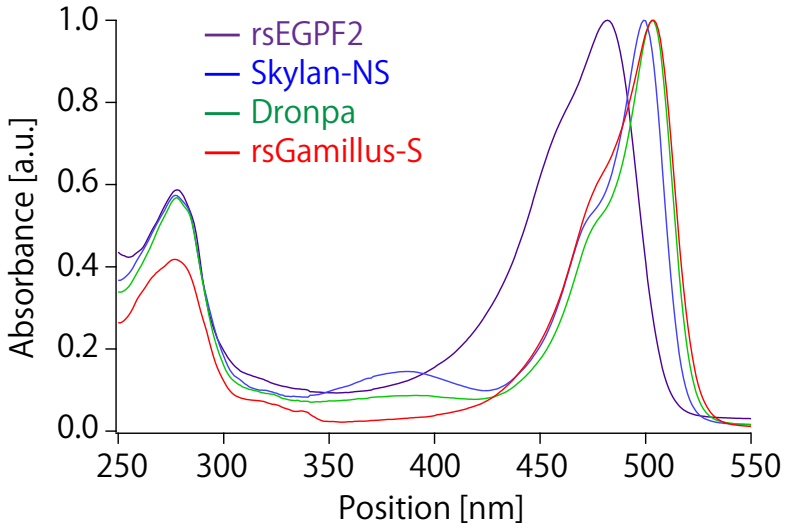

Figure S6. Absorption spectra of RSFPs at on-state. Purified RSFPs diluted in 20 mM HEPES (pH 7.5) were used for the measurement.

REFERENCES

(1) Richards, B.; Wolf, E.; Gabor, D. Electromagnetic Diffraction in Optical Systems, II. Structure of the Image Field in an Aplanatic System. *Proc. R. Soc. Lond. A Math. Phys. Sci.* **1959**, *253* (1274), 358–379.

(2) Bruce, A.; Johnson, A.; Lewis, J.; Raff, M.; Roberts, K.; Walter, P. *Molecular Biology of the Cell 5th Edition*; Garland Science, 2007.